Available at
http://pvamu.edu/aam
Appl. Appl. Math.
ISSN: 1932-9466

Applications and Applied Mathematics:
An International Journal
(AAM)

Vol. 12, Issue 2 (December 2017), pp. 946 - 967

Thermoelastic analysis of a nonhomogeneous hollow cylinder with internal heat generation

V. R. Manthena[a], N. K. Lamba[b], G. D. Kedar[a]

[a]Department of Mathematics
RTM Nagpur University
Nagpur, India

[b]Department of Mathematics
Shree Lemdeo Patil Mahavidyalaya
Nagpur, India
vkmanthena@gmail.com

Received: June 15, 2017; Accepted: November 24, 2017

Abstract

In the present paper, we have determined the heat conduction and thermal stresses of a hollow cylinder with inhomogeneous material properties and internal heat generation. All the material properties except Poisson's ratio and density are assumed to be given by a simple power law in axial direction. We have obtained the solution of the two dimensional heat conduction equation in the transient state in terms of Bessel's and trigonometric functions. The influence of inhomogeneity on the thermal and mechanical behavior is examined. Numerical computations are carried out for both homogeneous and nonhomogeneous cylinders and are represented graphically.

Keywords: Hollow Cylinder; Heat Conduction; Thermal Stresses; Inhomogeneity; Internal Heat Generation

AMS-MSC 2010 No.: 30E25; 34B05; 44A10; 74L05

1. Introduction

The thermoelastic behaviour of homogeneous and isotropic plates has attracted the focus of the researchers over the past few decades. The rationale for this interest is because of their sensible application in an exceeding sort of component parts and structures. As a result, the structural behaviour of isotropic circular plates has now been well understood, although new information continues to accumulate significantly in regard to the plates made of composites, functionally graded materials or heterogeneous metal materials. In general, nonhomogeneous materials are microscopically heterogeneous composites, which are usually made from a mixture of various

metallic elements. Nonhomogenous materials have a completely different spatial distribution of material properties and might be designed according to different applied science needs. Owing to their functional gradation for optimized design, nonhomogeneous material plates currently have absorbed significant attention as one of the most capable nominees for future intelligent composites in many engineering fields.

Thick cylinders are very important components which are extensively used in pressure vessels, accumulator shells, nuclear reactors, high-pressurized fluids. Aksoy et al. (2014) performed thermo elastic stress analysis on a cylinder made of laminated isotropic materials under thermomechanical loads. Al-Hajri and Kalla (2004) developed a new integral transform and its inversion involving combination of Bessel's function as a kernel and used it to solve mixed boundary value problems. . Awaji and Sivakumar (2001) presented a numerical technique for analyzing one-dimensional transient temperature distributions in a circular hollow cylinder composed of functionally graded ceramic–metal-based materials, without considering the temperature-dependent material properties. Ehteram et al. (2011) obtained an analytical solution for the temperature change and thermal stresses for the circumferential transient loading using finite Hankel and Fourier transform. Fu et al. (2014) presented the transient thermoelastic analysis in a long solid cylinder with a circumferential crack using the C–V heat conduction theory in which the outer surface of the cylinder is subjected to a sudden temperature change.

Hosseini and Akhlaghi (2009) obtained an analytical solution in transient thermoelasticity of functionally graded thick hollow cylinders. Hata (1982) studied thermal stresses in a nonhomogeneous plate and semi-infinite elastic solid under steady state temperature distribution. Jabbari et al. (2014) presented the buckling analysis of thermal loaded solid circular plate made of porous material by assuming the material properties of the porous plate vary across the thickness. Kassir (1972) investigated thermal stress problems in a thick plate and a semi-infinite body in nonhomogeneous solids. Kedar and Deshmukh (2015) studied inverse heat conduction problem to simultaneously determine unknown temperature and thermal deflection on the outer curved surface of a semi-infinite hollow circular cylinder from the knowledge of temperature distribution within the cylinder. Khobragade and Deshmukh (2005) developed an integral transform to determine temperature distribution in a thin circular plate, subjected to a partially distributed and axisymmetric heat supply on the curved surface. Kim and Noda (2002) adopted a Green's function approach based on the laminate theory for solving the two-dimensional unsteady temperature field (r, z) and the associated thermal stresses in an infinite hollow circular cylinder made of a FGM with radial-directionally dependent properties.

Kulkarni and Deshmukh (2007) determined quasi-static thermal stresses in a thick circular plate subjected to arbitrary initial temperature on the upper face with lower face at zero temperature and the fixed circular edge thermally insulated. Kulkarni and Deshmukh (2007) determined transient thermal stresses in a thick annular disc having zero initial temperature and subjected to arbitrary heat flux on the upper and lower surfaces. Recently Manthena et al. (2017) determined temperature distribution, displacement, and thermal stresses of a nonhomogeneous rectangular plate by assuming the material properties to vary by simple power law in *y* coordinate. Ootao (1995) used piecewise power law nonhomogeneity to study transient thermoelastic analysis of a functionally graded hollow circular disk. Ootao et al. (2012) developed a theoretical analysis of a three-dimensional transient thermal stress problem for a nonhomogeneous hollow circular cylinder. Sugano (1987) formulated a plane thermoelastic problem in a nonhomogeneous doubly connected

region and solved the system of fundamental equations using finite difference method. Sugano and Akashi (1989) studied transient plane thermal stress problem in a nonhomogeneous hollow circular plate by expressing Young's modulus and thermal conductivity in different power laws of radial coordinate. Sun and Li (2014) studied axisymmetrical thermal post-buckling of functionally graded material (FGM) circular plates with immovably clamped boundary and a transversely central point-space constraint. Tanigawa et al. (1997) studied elastic behavior for a medium with Kassir's nonhomogeneous material property.

Most of the literature cited above focuses on nonhomogeneous cylinders under steady state temperature distribution and all of them have considered homogeneous material properties. In fact, the problems with nonhomogeneous material properties are more practical and realistic, but due to the complexity and tedious calculations very few researchers studied such problems. In ample of cases, it is observed that, the heat production in solids have lead to various technical problems during mechanical applications in which heat is generated and rapidly transferred from their surface. Hence the study of thermoelastic behavior in nonhomogeneous materials with internal heat generation is needed. This problem deals with the determination of temperature and thermal behavior of a thick hollow cylinder with internal heat generation.

In the present article, we have considered a two-dimensional transient thermoelastic problem of a thick circular disc occupying the space $a \le r \le b,\ h_1 \le z \le h_2$, subjected to sectional heating on the curved surface. The material properties except Poisson's ratio and density are assumed to be nonhomogeneous given by a simple power law in axial direction. For theoretical treatment all physical and mechanical quantities are taken as dimensional, whereas for numerical analysis we have considered non-dimensional parameters. Numerical computations are carried out by considering both homogeneous and nonhomogeneous hollow cylinders.

2. Statement of the problem

2.1. Heat conduction equation

We consider the transient heat conduction equation with internal heat generation and initial and boundary conditions in a hollow cylinder given by

$$\frac{1}{r}\frac{\partial}{\partial r}\left(k(z)r\frac{\partial T}{\partial r}\right)+\frac{\partial}{\partial z}\left(k(z)\frac{\partial T}{\partial z}\right)+\Theta(r,z,t)=c(z)\,\rho\frac{\partial T}{\partial t}. \tag{1}$$

$$\begin{aligned}
&T = f_1(r, z), && at\ t = 0,\\
&e_1T + k_1\frac{\partial T}{\partial r} = 0, && at\ r = a,\ h_1 \le z \le h_2,\ t > 0,\\
&e_2T + k_2\frac{\partial T}{\partial r} = f_2(z, t), && at\ r = b,\ h_1 \le z \le h_2,\ t > 0,\\
&T = 0, && at\ z = h_1,\ a \le r \le b,\ t > 0,\\
&T = 0, && at\ z = h_2,\ a \le r \le b,\ t > 0,
\end{aligned} \tag{2}$$

where $f_1(r, z) = Q_0\delta(r - r_0)\delta(z - z_0)$, $f_2(z,t) = Q_1\delta(z - z_0)\cosh(\omega t)$, $k(z)$ and $c(z)$ are respectively, the thermal conductivity and calorific capacity of the material in the inhomogeneous region, ρ is the constant density, $\Theta(r,z,t)$ is the internal heat generation, e_1, e_2, k_1, k_2 are radiation constants.

2.2. Thermoelastic equations

The strain displacement relations, stress-strain relations and equilibrium condition are given by Hata (1982)

$$e_{rr} = \frac{\partial u}{\partial r}, \quad e_{\theta\theta} = \frac{u}{r}, \quad e_{zz} = \frac{\partial w}{\partial z}, \quad e_{rz} = \frac{1}{2}\left(\frac{\partial u}{\partial z} + \frac{\partial w}{\partial r}\right), \tag{3}$$

$$\begin{aligned}
\sigma_{rr} &= 2\mu(z)e_{rr} + \lambda(z)e - (3\lambda(z) + 2\mu(z))\alpha_T(z)T,\\
\sigma_{\theta\theta} &= 2\mu(z)e_{\theta\theta} + \lambda(z)e - (3\lambda(z) + 2\mu(z))\alpha_T(z)T,\\
\sigma_{zz} &= 2\mu(z)e_{zz} + \lambda(z)e - (3\lambda(z) + 2\mu(z))\alpha_T(z)T,\\
\sigma_{rz} &= 2\mu(z)e_{rz},
\end{aligned} \tag{4}$$

$$\begin{aligned}
\frac{\partial \sigma_{rr}}{\partial r} + \frac{\partial \tau_{rz}}{\partial z} + \frac{\sigma_{rr} - \sigma_{\theta\theta}}{r} &= 0,\\
\frac{\partial \sigma_{rz}}{\partial r} + \frac{\partial \sigma_{zz}}{\partial z} + \frac{\sigma_{rz}}{r} &= 0,
\end{aligned} \tag{5}$$

where $e_{rr}, e_{\theta\theta}, e_{zz}$ are the strain components $(e = e_{rr} + e_{\theta\theta} + e_{zz})$, $\lambda(z)$ and $\mu(z)$ are Lame constants, $\alpha_T(z)$ is the coefficient of thermal expansion.

Following Hata (1982), we assume that the shear modulus $\mu(z)$ and the coefficient of thermal expansion (CTE) $\alpha_T(z)$ vary in the axial direction given by

$$\mu(z) = \mu_0 z^p, \quad \alpha_T(z) = \alpha_0 z^p,$$

where μ_0 and α_0 are reference values of shear modulus and CTE, and $p \geq 0$ is related to Poisson's ratio υ by the relation $p\upsilon = 1 - 2\upsilon$, where υ is constant.

Using equations (3) and (4) in (5), the displacement equations of equilibrium are obtained as

$$\begin{aligned}
&\nabla^2 u - \frac{u}{r^2} + \frac{\nu}{1-2\upsilon}\frac{\partial e}{\partial r} + \frac{e_{rz}}{\mu(z)}\frac{\partial \mu(z)}{\partial z} + 2\frac{\partial e_{rz}}{\partial z} - \frac{1+\upsilon}{1-2\upsilon}\alpha_T(z)\frac{\partial T}{\partial r} = 0,\\
&\nabla^2 w + \frac{\nu}{1-2\upsilon}\frac{\partial e}{\partial z} + \frac{\partial e_{rr}}{\partial z} + \frac{e_{zz}}{\mu(z)}\frac{\partial \mu(z)}{\partial z} + \frac{e}{2\mu(z)}\frac{\partial \lambda(z)}{\partial z} - \frac{1+\upsilon}{1-2\upsilon}\left[\alpha_T(z)\frac{\partial T}{\partial z} + \theta\frac{\partial \alpha_T(z)}{\partial z}\right]\\
&-\frac{\alpha_T(z)}{2\mu(z)}\theta\left[3\frac{\partial \lambda(z)}{\partial z} + 2\frac{\partial \mu(z)}{\partial z}\right] + \frac{1}{r}\frac{\partial u}{\partial z} = 0,
\end{aligned} \tag{6}$$

where ∇^2 is given by

$$\nabla^2 = \frac{\partial^2}{\partial r^2} + \frac{1}{r}\frac{\partial}{\partial r} + \frac{\partial^2}{\partial z^2}. \tag{7}$$

The solution of equation (6) without body forces can be expressed by the Goodier's thermoelastic displacement potential ϕ and the Boussinesq harmonic functions φ and ψ as

$$\begin{aligned}
u &= \frac{\partial \varphi}{\partial r} + \frac{\partial \phi}{\partial r} + z\frac{\partial \psi}{\partial r},\\
w &= \frac{\partial \varphi}{\partial z} + \frac{\partial \phi}{\partial z} + z\frac{\partial \psi}{\partial z} - (3-4\nu)\psi,
\end{aligned} \tag{8}$$

in which the three functions must satisfy the conditions

$$\nabla^2\phi = K(z)\tau,\ \nabla^2\varphi = 0,\ \text{and}\ \ \nabla^2\psi = 0. \tag{9}$$

where $K(z) = \frac{(1+\nu)}{(1-\nu)}\alpha_T(z)$, is the restraint coefficient and $\tau = T - T_i$, in which T_i is the surrounding temperature. If we take

$$-\int(\varphi + z\psi)\,dz = M, \tag{10}$$

in the above equation (8), Michell's function M may be used instead of Boussinesq harmonic functions φ and ψ. Hence, equation (8) reduces to

$$\begin{aligned}
u &= \frac{\partial \varphi}{\partial r} - \frac{\partial^2 M}{\partial r\,\partial z},\\
w &= \frac{\partial \varphi}{\partial z} + 2(1-\nu)\nabla^2 M - \frac{\partial^2 M}{\partial z^2},
\end{aligned} \tag{11}$$

in which Michell's function M must satisfy the condition

$$\nabla^2\nabla^2 M = 0. \tag{12}$$

Now by using equation (11) in equations (4) and (6), the results for thermoelastic fields are obtained as

$$\nabla^2\phi-\frac{\partial}{\partial z}(\nabla^2 M)-\frac{1}{r^2}(\phi-\frac{\partial M}{\partial z})-\frac{1+\nu}{1-2\nu}\alpha_T(z)T=0, \tag{13}$$

$$\begin{aligned}\nabla^2\varphi+2(1-\nu)\left[\nabla^2 M+\frac{\partial}{\partial z}(\nabla^2 M)+\frac{\partial}{\partial r}(\nabla^2 M)\right]+2(1-\nu)\left[\frac{2-r}{r^3}\frac{\partial M}{\partial r}-\frac{2}{r^2}\frac{\partial^2 M}{\partial r^2}\right]\\ -\frac{1+\nu}{1-2\nu}\alpha_T(z)T-(3\lambda+2\mu)\frac{\alpha_T(z)}{2\mu(z)}T+\frac{1}{r}\left[\frac{\partial\varphi}{\partial r}-\frac{\partial^2 M}{\partial r\,\partial z}\right]=0.\end{aligned} \tag{14}$$

The corresponding stresses are given by

$$\begin{aligned}\sigma_{rr}&=2\mu(z)\frac{\partial}{\partial r}\left(\frac{\partial\phi}{\partial r}-\frac{\partial^2 M}{\partial r\,\partial z}\right)+\lambda(z)\left[\nabla^2\phi+(1-2\nu)\frac{\partial}{\partial z}(\nabla^2 M)\right]-(3\lambda(z)+2\mu(z))\alpha_T(z)T,\\ \sigma_{\theta\theta}&=2\mu(z)\frac{1}{r}\left(\frac{\partial\phi}{\partial r}-\frac{\partial^2 M}{\partial r\,\partial z}\right)+\lambda(z)\left[\nabla^2\phi+(1-2\nu)\frac{\partial}{\partial z}(\nabla^2 M)\right]-(3\lambda(z)+2\mu(z))\alpha_T(z)T,\\ \sigma_{zz}&=2\mu(z)\frac{\partial}{\partial z}\left(\frac{\partial\phi}{\partial z}+2(1-\nu)\nabla^2 M-\frac{\partial^2 M}{\partial z^2}\right)+\lambda(z)\left[\nabla^2\phi+(1-2\nu)\frac{\partial}{\partial z}(\nabla^2 M)\right]\\ &\quad-(3\lambda(z)+2\mu(z))\alpha_T(z)T,\\ \sigma_{rz}&=\mu(z)\left[\frac{\partial}{\partial z}\left(\frac{\partial\phi}{\partial r}-\frac{\partial^2 M}{\partial r\,\partial z}\right)+\frac{\partial}{\partial r}\left(\frac{\partial\phi}{\partial z}+2(1-\nu)\nabla^2 M-\frac{\partial^2 M}{\partial z^2}\right)\right].\end{aligned} \tag{15}$$

The boundary conditions on the traction free surface stress functions are

$$\sigma_{rr}\big|_{r=a}=\sigma_{rr}\big|_{r=b}=0. \tag{16}$$

Equations (1) to (16) constitute the mathematical formulation of the problem.

3 Solution of the problem

3.1. Heat conduction equation

From equation (1), we have

$$k(z)\left(\frac{\partial^2 T}{\partial r^2}+\frac{1}{r}\frac{\partial T}{\partial r}\right)+k(z)\frac{\partial^2 T}{\partial z^2}+\frac{\partial T}{\partial z}k'(z)+\Theta(r,z,t)=c(z)\,\rho\frac{\partial T}{\partial t}. \tag{17}$$

The initial and boundary conditions are

$$\begin{aligned} &T = f_1(r, z), && at\ t = 0, \\ &e_1 T + k_1 \frac{\partial T}{\partial r} = 0, && at\ r = a,\ h_1 \le z \le h_2,\ t > 0, \\ &e_2 T + k_2 \frac{\partial T}{\partial r} = f_2(z, t), && at\ r = b,\ h_1 \le z \le h_2,\ t > 0, \\ &T = 0, && at\ z = h_1,\ a \le r \le b,\ t > 0, \\ &T = 0, && at\ z = h_2,\ a \le r \le b,\ t > 0. \end{aligned} \tag{18}$$

For the sake of brevity, we consider

$$\begin{aligned} &k(z) = k_0 z^p,\ c(z) = c_0 z^p,\ \rho = \rho_0, \\ &\Theta(r, z, t) = k_0 z^{((1+p)/2)} \Theta_1(r, t),\ \Theta_1(r, t) = \delta(r - r_0)\,\delta(t - t_0). \end{aligned} \tag{19}$$

Here, k_0, c_0 and ρ_0 are the reference values of thermal conductivity, calorific capacity and density, respectively. Using equation (19) in (17), we obtain

$$\left(\frac{\partial^2 T}{\partial r^2} + \frac{1}{r}\frac{\partial T}{\partial r}\right) + \left(\frac{\partial^2 T}{\partial z^2} + \frac{p}{z}\frac{\partial T}{\partial z}\right) + z^{((1-p)/2)} \Theta_1(r, t) = \frac{1}{\kappa}\frac{\partial T}{\partial t}, \tag{20}$$

where $\kappa = (k_0 / c_0 \rho_0)$ and

$$\begin{aligned} &T = Q_0 \delta(r - r_0)\,\delta(z - z_0), && at\ t = 0, \\ &e_1 T + k_1 \frac{\partial T}{\partial r} = 0, && at\ r = a,\ h_1 \le z \le h_2,\ t > 0, \\ &e_2 T + k_2 \frac{\partial T}{\partial r} = Q_1 \delta(z - z_0)\cosh(\omega t), && at\ r = b,\ h_1 \le z \le h_2,\ t > 0, \\ &T = 0, && at\ z = h_1,\ a \le r \le b,\ t > 0, \\ &T = 0, && at\ z = h_2,\ a \le r \le b,\ t > 0. \end{aligned} \tag{21}$$

To remove p from the numerator of equation (20), we use the variable transformation $T = z^{((1-p)/2)}\,\theta(r, z, t)$. Hence, equation (20) reduces to

$$\left(\frac{\partial^2 \theta}{\partial r^2} + \frac{1}{r}\frac{\partial \theta}{\partial r}\right) + \left(\frac{\partial^2 \theta}{\partial z^2} + \frac{1}{z}\frac{\partial \theta}{\partial z} + \frac{\gamma^2}{z^2}\theta\right) + \Theta_1(r, t) = \frac{1}{\kappa}\frac{\partial \theta}{\partial t}, \tag{22}$$

where $\gamma^2 = ((p-1)/2).$

The initial and boundary conditions are

$$\begin{aligned}
&\theta = Q_0 z^{((p-1)/2)} \delta(r-r_0)\,\delta(z-z_0), && at\ t=0,\\
&e_1\theta + k_1 \frac{\partial\theta}{\partial r} = 0, && at\ r=a,\ h_1 \le z \le h_2,\ t>0,\\
&e_2\theta + k_2 \frac{\partial\theta}{\partial r} = Q_1 z^{((p-1)/2)} \delta(z-z_0)\cosh(\omega t), && at\ r=b,\ h_1 \le z \le h_2,\ t>0,\\
&\theta = 0, && at\ z=h_1,\ a \le r \le b,\ t>0,\\
&\theta = 0, && at\ z=h_2,\ a \le r \le b,\ t>0.
\end{aligned} \tag{23}$$

To solve the differential equation (22) using integral transform technique, we introduce the extended integral transform Al-Hajri and Kalla (2004) of order i over the variable z as given below (Refer Appendix A).

$$T[f(z),a,b;\gamma_i] = \bar{f}(\gamma_i) = \int_{h1}^{h2} z\, f(z) S(\gamma_i z)\, dz. \tag{24}$$

Here, $S(\gamma_i z)$ is the kernel of the transform given by

$$S(\gamma_i z) = Z_i \cos(\gamma_i \log z) - W_i \sin(\gamma_i \log z),\ z>0, \tag{25}$$

where

$$Z_i = \sin(\gamma_i \log h_1) + \sin(\gamma_i \log h_2),\quad W_i = \cos(\gamma_i \log h_1) + \cos(\gamma_i \log h_2), \text{and } \gamma_i (i = 1,2,3,...)$$

are the real and positive roots of the transcendental equation

$$\sin(\gamma \log h_1)\cos(\gamma \log h_2) - \sin(\gamma \log h_2)\cos(\gamma \log h_1) = 0. \tag{26}$$

The inversion formula is

$$f(z) = \sum_{i=1}^{\infty} \frac{\bar{f}(\gamma_i)}{S(\gamma_i)} S(\gamma_i z), \tag{27}$$

where

$$\int_{h1}^{h2} z\, S(\gamma_i z) S(\gamma_j z)\, dz = \begin{cases} S(\gamma_i), & i=j,\\ 0, & i \ne j. \end{cases} \tag{28}$$

Hence, equations (22) and (23) become

$$\left(\frac{\partial^2\bar{\theta}}{\partial r^2}+\frac{1}{r}\frac{\partial\bar{\theta}}{\partial r}\right)-\gamma_i^2\bar{\theta}+\bar{\Theta}_1(r,t)=\frac{1}{\kappa}\frac{\partial\bar{\theta}}{\partial t}. \tag{29}$$

$$\begin{aligned}
&\bar{\theta}=Q_0 g_0\delta(r-r_0), && at\ t=0,\\
&e_1\bar{\theta}+k_1\frac{\partial\bar{\theta}}{\partial r}=0, && at\ r=a,\ h_1\le z\le h_2,\ t>0,\\
&e_2\bar{\theta}+k_2\frac{\partial\bar{\theta}}{\partial r}=Q_1 g_0\cosh(\omega t), && at\ r=b,\ h_1\le z\le h_2,\ t>0,
\end{aligned} \tag{30}$$

where

$$g_0=\int_{h1}^{h2} z^{((p+1)/2)}\delta(z-z_0)S(\gamma_i z)\,dz,\quad \bar{\Theta}_1(r,t)=\delta(r-r_0)\,\delta(t-t_0).$$

We use the transform given in Al-Hajri and Kalla (2004) to solve equation (29) and use the boundary conditions given by equation (30), and obtain

$$\frac{\partial\bar{\bar{\theta}}}{\partial t}+A_1\bar{\bar{\theta}}=A_2\cosh(\omega t)+A_3\delta(t-t_0), \tag{31}$$

$$\bar{\bar{\theta}}=Q_0 g_0 r_0 M(q_n r_0),\quad at\ t=0, \tag{32}$$

where

$$A_1=\kappa(q_n^2+\gamma_i^2),\quad A_2=\frac{\kappa h_1}{k_2}M(q_n h_1)Q_1 g_0,\quad A_3=\kappa r_0 M(q_n r_0).$$

Here, $M(q_n r)$ is the kernel of the transformation given by

$$M(q_n r)=[B(q_n a,e_1,k_1)+B(q_n b,e_2,k_2)]J_0(q_n r)-[A(q_n a,e_1,k_1)+A(q_n b,e_2,k_2)]Y_0(q_n r),$$

in which

$$\begin{aligned}
&A(q_n r,e_n,k_n)=e_n J_0(q_n r)+k_n q_n J_0'(q_n r);\ n=1,2;\ r=a,b,\\
&B(q_n r,e_n,k_n)=e_n Y_0(q_n r)+k_n q_n Y_0'(q_n r);\ n=1,2;\ r=a,b.
\end{aligned}$$

Here, J_0 and Y_0 are Bessel's function of first kind and second kind, respectively and q_n are the positive roots of the transcendental equation

$$B(q_n a, e_1, k_1) \times A(q_n b, e_2, k_2) - A(q_n a, e_1, k_1) \times B(q_n b, e_2, k_2) = 0.$$

Applying Laplace transform and its inverse on equation (31) by using the initial condition given in equation (32), we obtain

$$\bar{\bar{\theta}}(n,t) = E_1 \exp(-A_1 t) + E_2 \exp(-\omega t) + E_3 \exp(\omega t) + A_3 \exp(-A_1(t-t_0))\theta^*(t-t_0), \tag{33}$$

where

$$E_1 = \frac{A_1 A_2}{\omega^2 - A_1^2} + A_4,\ E_2 = \frac{A_2}{2A_1 - 2\omega},\ E_3 = \frac{A_2}{2\omega + 2A_1},\ A_4 = Q_0 g_0 r_0 M(q_n r_0).$$

Here, $\theta^*(t-t_0)$ is the Heaviside Theta function given by

$$\theta^*(t-t_0) = \begin{cases} 0, & t < t_0, \\ 1, & t > t_0. \end{cases}$$

Applying inverse transform on equation (33), we obtain

$$\bar{\theta}(r,t) = \sum_{n=1}^{\infty} \frac{E_1 \exp(-A_1 t) + E_2 \exp(-\omega t) + E_3 \exp(\omega t) + A_3 \exp(-A_1(t-t_0))\theta^*(t-t_0)}{M(q_n)} \times M(q_n r). \tag{34}$$

Applying inverse transform defined in equation (27) on the above equation (34), we obtain

$$\theta(r,z,t) = \sum_{i=1}^{\infty} \sum_{n=1}^{\infty} \frac{\bar{\theta}(r,t)}{S(\gamma_i)} \times S(\gamma_i z),\ z > 0. \tag{35}$$

Using equation (35) in the equation $T = z^{((1-p)/2)}\theta(r,z,t)$, we obtain

$$T(r,z,t) = \sum_{i=1}^{\infty} \sum_{n=1}^{\infty} \{\xi_1 \times \xi_2(t) \times [\xi_3 J_0(q_n r) - \xi_4 Y_0(q_n r)] \times g_1(z)\}, \tag{36}$$

where

$$\xi_1 = 1/[M(q_n) \times S(\gamma_i)],$$
$$\xi_2(t) = E_1 \exp(-A_1 t) + E_2 \exp(-\omega t) + E_3 \exp(\omega t) + A_3 \exp(-A_1(t-t_0))\theta^*(t-t_0),$$
$$\xi_3 = [B(q_n h_1, e_1, k_1) + B(q_n h_2, e_2, k_2)],\ \xi_4 = [A(q_n h_1, e_1, k_1) + A(q_n h_2, e_2, k_2)],$$
$$g_1(z) = z^{((1-p)/2)} \times S(\gamma_i z),\ z > 0.$$

3.2. Thermoelastic equations

Referring to the heat conduction equation (17) and its solution given by equation (36), the solution for the Goodier's thermoelastic displacement potential ϕ governed by equation (9) is obtained as

$$\phi = \sum_{i=1}^{\infty} \sum_{n=1}^{\infty} \frac{K(z)(T^2(r,z,t) - T_i(r,z))}{\xi_1 \times \xi_2(t) \times [\xi_3 J_0(q_n r) - \xi_4 Y_0(q_n r)] \times [-q_n^2 g_1(z) + g_1''(z)]}. \quad (37)$$

Similarly, the solution for Michell's function M assumed so as to satisfy the governed condition of equation (12) is obtained as

$$M = \sum_{i=1}^{\infty} \sum_{n=1}^{\infty} \{z^{((1-\alpha)/2)} \times [\cos(\log z) - \sin(\log z)] \exp(\omega t)[C_m J_0(q_n r) + D_m Y_0(q_n r)]\}, \quad (38)$$

where C_m and D_m are constants.

Now, in order to obtain the displacement components, we substitute the values of ϕ and M in equation (11), and obtain

$$u = \sum_{i=1}^{\infty} \sum_{n=1}^{\infty} \{\phi_{,r} + q_n g_2'(z) \exp(\omega t)[C_m J_1(q_n r) + D_m Y_1(q_n r)]\}, \quad (39)$$

$$\begin{aligned} w = \sum_{i=1}^{\infty} \sum_{n=1}^{\infty} \{&\varphi_{,z} + (2\nu - 2) q_n^2 [g_2(z) \exp(\omega t)[C_m J_0(q_n r) + D_m Y_0(q_n r)]] \\ &+ (1 - 2\nu)[g_2''(z) \exp(\omega t)[C_m J_0(q_n r) + D_m Y_0(q_n r)]]\}, \end{aligned} \quad (40)$$

where

$$g_2(z) = z^{((1-\alpha)/2)} \times [\cos(\log z) - \sin(\log z)].$$

Using the displacement components given by equations (39) and (40) in equation (15), the components of stresses can be obtained.

Also by using the traction free conditions given by equation (16) the constants C_m and D_m can be determined.

Since the equations of stresses and constants C_m and D_m obtained so are very large, hence we have not mentioned them here. However numerical computations are carried out by using Mathematica software.

4. Numerical results and discussion

The numerical computations have been carried out for a mixture of Copper and Tin metals (Hata 1982) in the ratio 70:30 respectively, with non-dimensional variables as given below.

$$\Delta = \frac{T}{T_R}\ , \quad \eta = \frac{r}{a}\ , \quad \zeta = \frac{z-h_1}{a}\ , \quad \tau = \frac{\kappa t}{a^2}\ , \quad \bar{h} = \frac{h}{a}\ , \quad (\bar{u},\bar{w}) = \frac{(u,w)}{\alpha_0 T_R a}\ ,$$
$$(\bar{\sigma}_{rr},\bar{\sigma}_{\theta\theta},\bar{\sigma}_{zz},\bar{\sigma}_{rz}) = \frac{(\sigma_{rr},\sigma_{\theta\theta},\sigma_{zz},\sigma_{rz})}{E\alpha_0\theta_R},$$

with parameters

$$a = 1\,cm,\ b = 3\,cm,\ h_1 = 2cm, h_2 = 5cm,\ r_0 = 1.5\,cm,\ t_0 = 2\ \text{sec},\ t = 3\ \text{sec},$$

reference temperature $T_R = 32^o C$, thermal expansion coefficient $\alpha_0 = 17\times10^{-6}/^o C$, $\kappa = 1.11cm^2/\text{sec}$. Here, 2.6, 4.7, 6.1, 8.2, 11.3, 14.5, 17.3, 21.1, 25.3, 29.9, 36.3, 42.7, 49.1, 56.6, 64.2 are the real and positive roots of the transcendental equation

$$B(q_i a, e_1, k_1)\times A(q_i b, e_2, k_2) - A(q_i a, e_1, k_1)\times B(q_i b, e_2, k_2) = 0\ .$$

The Young's modulus E is given by the following equation (JSME 1980)

$$E(x) = (0.1174 - 0.2246x - 1.347x^2 - 5.814x^3 + 8.495x^4)\times 9.8\times10^7\ N/cm^2.$$

Here. x: weight of tin $\div 100$, $0 \le x \le 0.3$. Let $x = 0.3$, then $E = 4.41\times10^7\ N/cm^2$.

For different values of parameter p, the Poisson's ratio ν and Shear modulus μ_0 are calculated by using the formula $p\nu = 1 - 2\nu$, $\mu_0 = \dfrac{E}{2(1+\nu)}$.

(1) For Homogeneous Cylinder: $p = 0$, Poisson's ratio $\nu = 0.5$, Shear modulus $\mu_0 = 1.47\times10^7\ N/cm^2$.

(2) For Nonhomogeneous Cylinder: $p = 1.5$, Poisson's ratio $\nu = 0.286$, Shear modulus $\mu_0 = 1.715\times10^7\ N/cm^2$.

Figure 1 shows the variation of dimensionless temperature in radial direction for different values of dimensionless thickness $\zeta = 0.5, 1.5, 2, 2.5, 3$. From the graph it is seen that the nature is sinusoidal. The temperature has a finite value at the outer radius due to internal heat generation, which is gradually decreasing in the region $2.5 \le \eta \le 3$ and increasing towards the inner radius for both homogeneous and nonhomogeneous cylinders. The magnitude of temperature is high at the lower surface due to sectional heating, and is gradually decreasing towards the upper surface. Also the magnitude of temperature is high for homogeneous cylinder as compared to nonhomogeneous cylinder.

Figure 2 shows the variation of dimensionless displacement $\overline{w}$ in radial direction for different values of dimensionless thickness ζ. It is seen that the displacement is more at the outer radius and is gradually decreasing in the region $2 \le \eta \le 3$ for both homogeneous and nonhomogeneous cylinders.

Figure 3 shows the variation of dimensionless radial stress in radial direction for different values of dimensionless thickness ζ. It is seen that the nature is dome shaped. The radial stress is compressive throughout the cylinder. It is gradually decreasing in the region $2.1 \le \eta \le 3$ and increasing towards the inner radius. Due to the accumulation of thermal energy, the magnitude is more towards the inner radius. Also the radial stress is zero at both the radial ends (for both homogeneous and nonhomogeneous cylinders), which agrees with the prescribed traction free boundary conditions.

Figure 4 shows the variation of dimensionless tangential stress in radial direction for different values of dimensionless thickness ζ. For homogeneous cylinder, the tangential stress is tensile from the outer to the inner radius till $\eta = 1.1$ and compressive at the end for all values of ζ except $\zeta = 2.5$. For nonhomogeneous cylinder, the magnitude of crest and trough is high in the outer radius which gradually decreases towards the inner radius.

Figure 5 shows the variation of dimensionless axial stress in radial direction for different values of dimensionless thickness ζ. The axial stress is converging to zero at the central region for both homogeneous cylinder and nonhomogeneous cylinders and is tensile in nature for $2.1 \le \eta \le 3$ and $1 \le \eta \le 1.5$, whereas compressive for $1.5 \le \eta \le 2.1$. Also the magnitude of crest and trough is high at the lower surface which gradually decreases towards the inner surface.

Figure 6 shows the variation of dimensionless shear stress in radial direction for different values of dimensionless thickness ζ. The shear stress is tensile in nature for $1.8 \le \eta \le 2.6$ and $1 \le \eta \le 1.2$, whereas compressive for $1 \le \eta \le 1.8$ and $2.6 \le \eta \le 3$. Also the magnitude of shear stress is more for homogeneous cylinder as compared to nonhomogeneous cylinder. The figures (1 to 6) on the left are of homogeneous hollow cylinder and those on the right are of nonhomogeneous hollow cylinder.

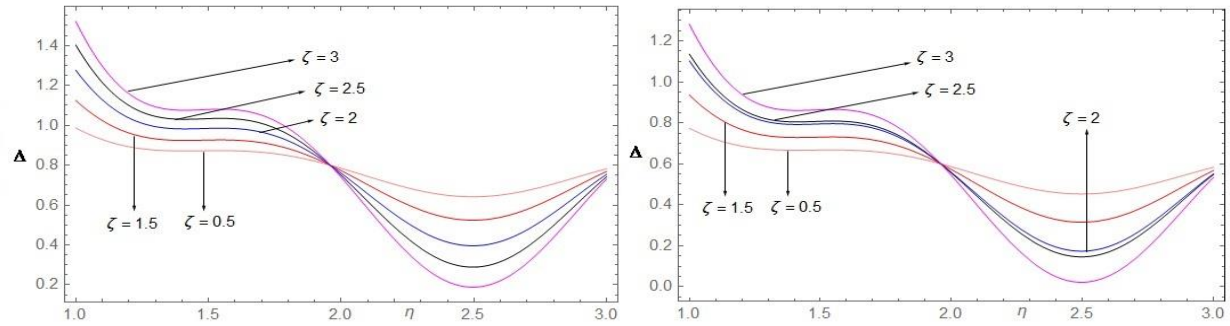

Homogeneous Hollow Cylinder **Nonhomogeneous Hollow Cylinder**

Figure 1. Variation of dimensionless temperature with η and ζ

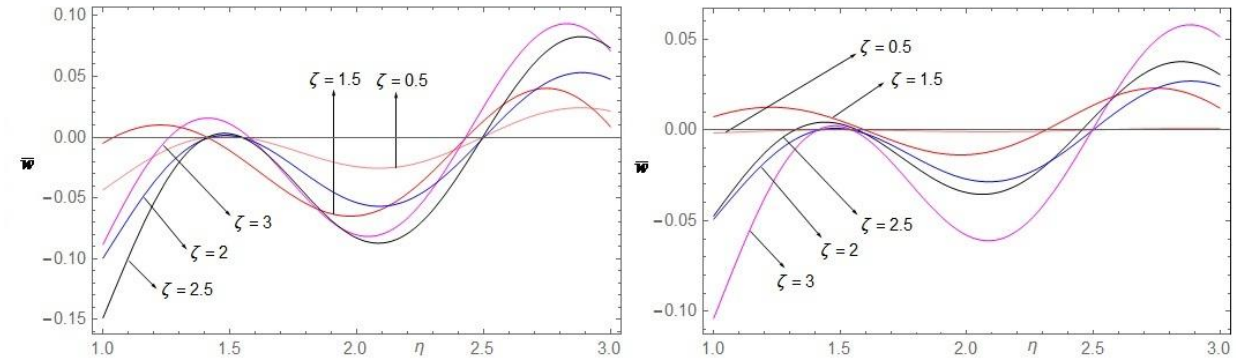

Figure 2. Variation of dimensionless displacement $\bar{w}$ with η and ζ

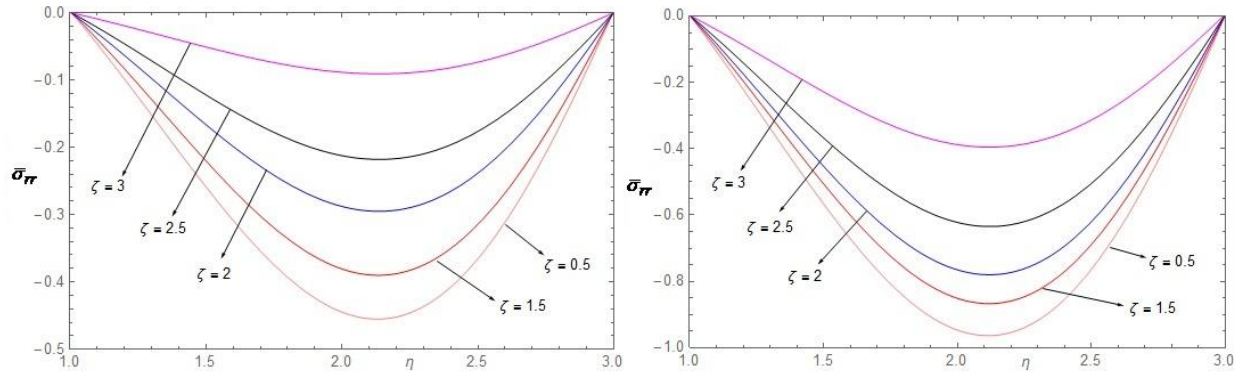

Figure 3. Variation of dimensionless radial stress with η and ζ

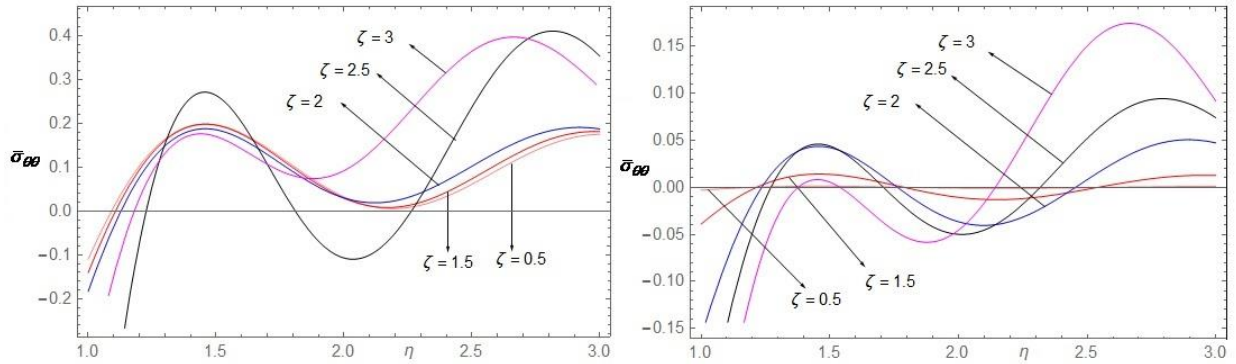

Figure 4. Variation of dimensionless tangential stress with η and ζ

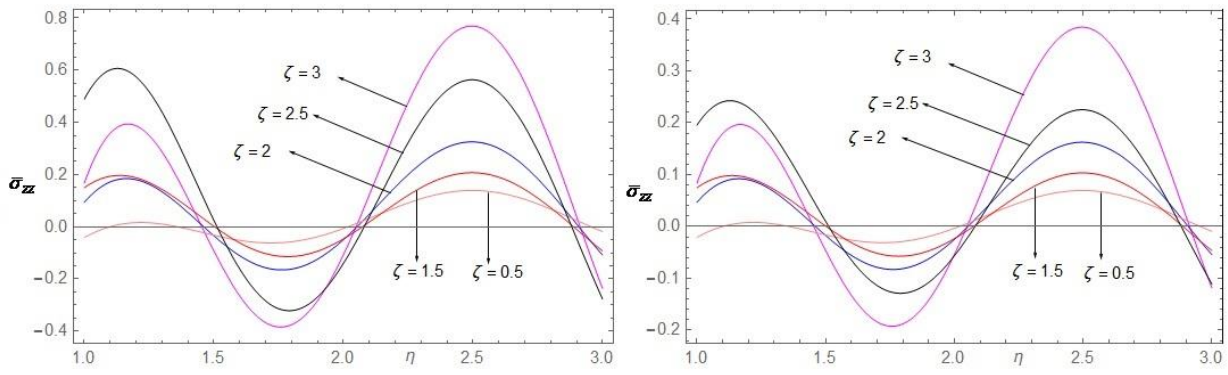

Figure 5. Variation of dimensionless axial stress with η and ζ

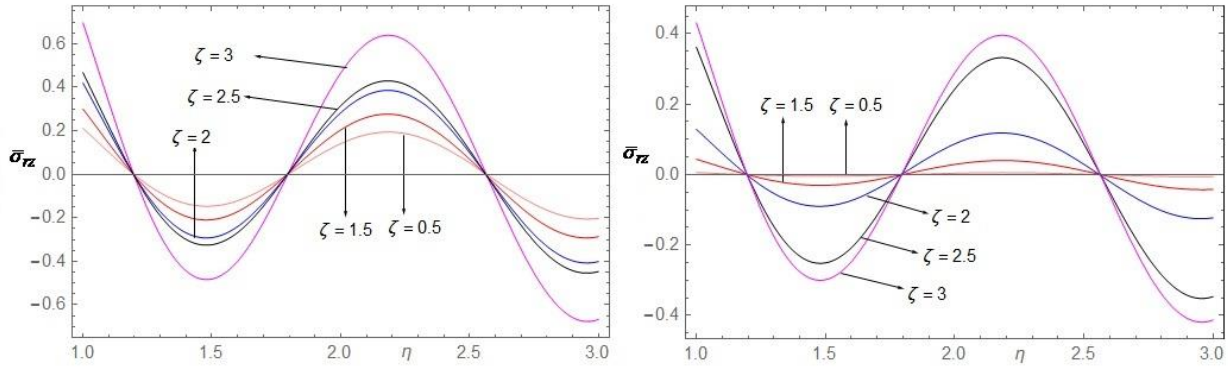

Figure 6. Variation of dimensionless shear stress with η and ζ

Figure 7 shows the variation of dimensionless temperature in radial direction for different values of inhomogeneity parameter $p = 0, 1, 2, 3, 4$. It is seen that the temperature has a finite value at the outer radius due to internal heat generation, which is gradually increasing in the region $2.5 \le \eta \le 3$ and then decreasing towards the inner radius. With increase in the inhomogeneity parameter p, the magnitude of temperature is decreasing.

Figure 8 shows the variation of dimensionless displacement $\overline{w}$ in radial direction for different values of p. It is seen that the displacement is more at the outer radius and is gradually decreasing till $\eta = 2$ and then increasing till $\eta = 1.4$.

Figure 9 shows the variation of dimensionless radial stress in radial direction for different values of p. It is seen that the nature is bell shaped. The radial stress is compressive throughout the cylinder. With increase in the inhomogeneity parameter p, the absolute value of radial stress is decreasing.

Figures 10, 11 and 12 show the variation of dimensionless tangential stress, axial stress and shear stress respectively in radial direction for different values of p. With increase in the inhomogeneity

parameter p, it is seen that the magnitude of axial stress in less as compared to that of tangential stress and shear stress. The axial stress is compressive throughout, whereas crest and trough are observed in tangential stress and shear stress.

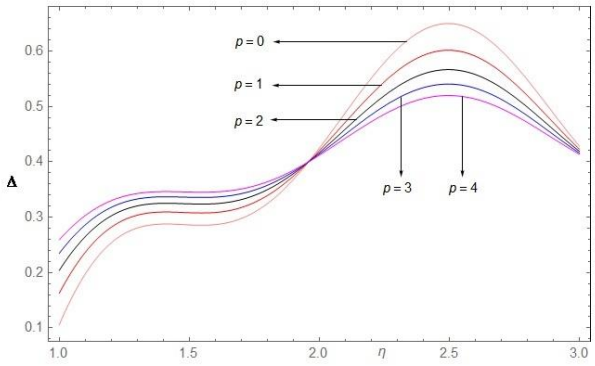

Figure 7. Variation of dimensionless temperature with η for different values of p

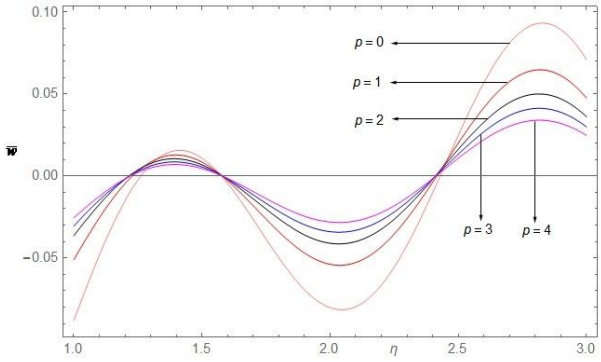

Figure 8. Variation of dimensionless displacement $\overline{w}$ with η for different values of p

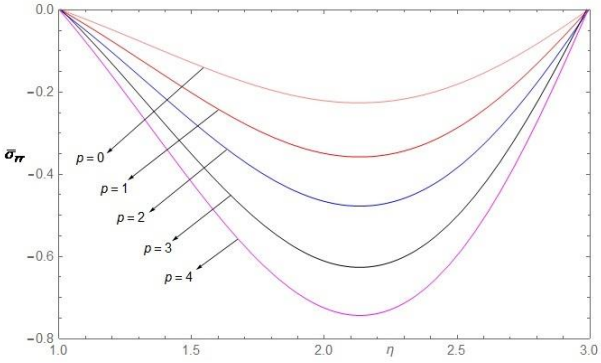

Figure 9. Variation of dimensionless radial stress with η for different values of p

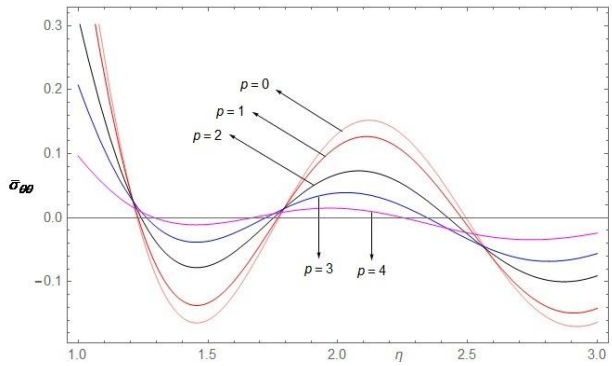

Figure 710 Variation of dimensionless tangential stress with η for different values of p

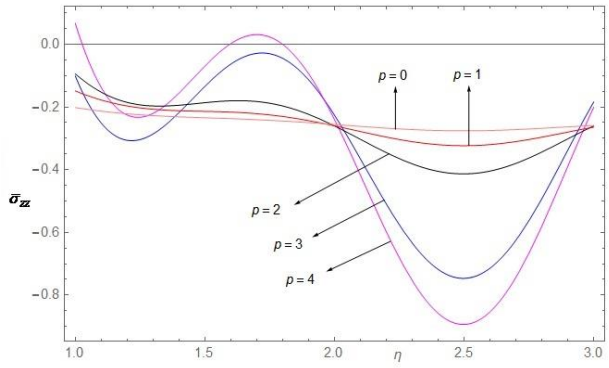

Figure 11. Variation of dimensionless axial stress with η for different values of p

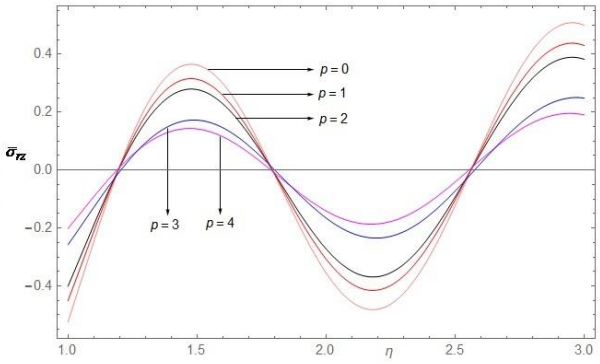

Figure 12. Variation of dimensionless shear stress with η for different values of p

5. Conclusion

In the present paper, we have determined temperature distribution with internal heat generation and thermal stresses in a thick hollow cylinder subjected to sectional heating on the curved surface.

The material properties except Poisson's ratio and density are considered to vary by simple power law along axial direction. We have obtained the solution for transient two-dimensional conductivity equation with internal heat generation and its associated thermal stresses for a thick hollow cylinder with inhomogeneous material properties. The solutions are obtained in the form of Bessel's and trigonometric functions. Numerical computations are carried out for a mixture of copper and tin metals in the ratio 70:30 respectively and the transient state temperature field and thermal stresses are examined. Furthermore the influence of inhomogeneity grading is investigated by changing parameter p.

During our investigation, the following results are obtained.

(i) The nature of temperature, displacement and all stresses is observed to be sinusoidal when plotted along radial direction for different values of dimensionless thickness ζ.
(ii) The magnitude of temperature, displacement and all stresses is found to be high for homogeneous cylinder as compared to nonhomogeneous cylinder.
(iii) By increasing the inhomogeneity parameter p, it is observed that the absolute values of temperature and displacement are high near the outer radius due to external sectional heating at the outer edge, and are gradually decreasing towards the inner radius.
(iv) By increasing the inhomogeneity parameter p, it is observed that
    (a) The magnitude of radial and axial stress at $p = 4$ attains minimum compared to $p = 0$, due to compressive force at the central region along radial direction.
    (b) The magnitude of tangential and shear stress for $p = 0$ at $\eta = 1.5, 3,$ attains minimum compared to $p = 4$, due to compressive force at the central region along radial direction.

Hence, we conclude that, fluctuations in the temperature distribution as well as thermoelastic quantities are observed in the neighborhood region of the internal heat generation, due to the presence of internal heat generation.

REFERENCES

Aksoy, Ş., Kurşun, A., Çetin, E., and Haboğlu, M. R. (2014). Stress Analysis of Laminated Cylinders Subject to the Thermomechanical Loads, International Journal of Mechanical, Aerospace, Industrial, Mechatronic and Manufacturing Engineering, 8(2), 244-249.

Al-Hajri, M. and Kalla, S. L. (2004). On an integral transform involving Bessel functions, Proceedings of the international conference on Mathematics and its applications, Kuwait, April 5-7.

Awaji, H. and Sivakumar, R. (2001). Temperature and Stress Distributions in a Hollow Cylinder of Functionally Graded Material: The Case of Temperature-Independent Material Properties, Journal of the American Ceramic Society, 84(5), 1059-1065.

Birkoff, G. and Rota, G. C. (1989). Ordinary differential equations, Wiley, New York.

Edited by Japan Soc. of Mech. Eng., Elastic coefficient of Metallic materials, Japan Soc. of Mech. Eng., Japan, October 1980 (in Japanese).

Ehteram, M. A., Sadighi, M., and Tabrizi, H. B. (2011). Analytical solution for thermal stresses of laminated hollow cylinders under transient nonuniform thermal loading, Mechanika, 17(1), 30-37.

Fu, J., Chen, Z., Qian, L., and Hu, K. (2014). Transient Thermoelastic Analysis of a Solid Cylinder Containing a Circumferential Crack Using the C–V Heat Conduction Model, Journal of Thermal Stresses, 37(11), 1324-1345.

Hosseini, S. M. and Akhlaghi, M. (2009). Analytical solution in transient thermoelasticity of functionally graded thick hollow cylinders, Math. Methods Appl. Sci., 32(15), 2019-2034.

Hata, T. (1982). Thermal stresses in a nonhomogeneous thick plate under steady distribution of temperature, Journal of Thermal Stresses, 5(1), 1-11.

Jabbari, M., Hashemitaheri, M., Mojahedin, A., and Eslami, M. R. (2014). Thermal Buckling Analysis of Functionally Graded Thin Circular Plate Made of Saturated Porous Materials, Journal of Thermal Stresses, 37(2), 202-220.

Kassir, M. K. (1972). Boussinesq Problems for Nonhomogeneous Solid, Proc. Am. Soc. Civ. Eng., J. Eng. Mech. Div., 98(2),457-470.

Kedar, G. D. and Deshmukh, K. C. (2015). Inverse Heat Conduction Problem in a Semi-infinite Hollow Cylinder and its Thermal Deflection by Quasi-static Approach, International Journal of Applied Mathematics and Computation, 6(2), 15-21.

Khobragade, N. L. and Deshmukh, K. C. (2005). Thermal deformation in a thin circular plate due to a partially distributed heat supply, Sadhana, 30(4), 555-563.

Kim, K. S. and Noda, N. (2002). Green's function approach to unsteady thermal stresses in an infinite hollow cylinder of functionally graded material, Acta Mechanica, 156(3), 145-161.

Kulkarni, V. S. and Deshmukh, K. C. (2007). Quasi-static thermal stresses in a thick circular plate, Applied mathematical modelling, 31(8), 1479-1488.

Kulkarni, V. S. and Deshmukh, K. C. (2007). Quasi-static transient thermal stresses in a thick annular disc, Sadhana, 32(5), 561-575.

Manthena, V. R., Lamba, N. K., and Kedar, G. D. (2017). Transient thermoelastic problem of a nonhomogeneous rectangular plate, Journal of Thermal Stresses, 40(5), 627-640.

Ootao, Y., Akai, T., and Tanigawa, Y. (1995). Three-dimensional transient thermal stress analysis of a nonhomogeneous hollow circular cylinder due to a moving heat generation in the axial direction, Journal of Thermal Stresses, 18(5), 497-512.

Ootao, Y. (2012). Transient thermoelastic analysis for a functionally graded hollow circular disk with piecewise power law nonhomogeneity, Journal of Thermal Stresses, 35(1), 75-90.

Sugano, Y. (1987). Transient thermal stresses in a nonhomogeneous doubly connected region, Japan Soc. Mech. Eng., 53(489), 941–946 (in Japanese).

Sugano, Y. and Akashi, K. (1989). An analytical solution of unaxisymmetric transient thermal stresses in a nonhomogeneous hollow circular plate, Trans. Jpn. Soc. Mech. Eng., 55(509), 89-95.

Sun, Y. and Li, S. R. (2014). Thermal Post-Buckling of Functionally Graded Material Circular Plates Subjected to Transverse Point-Space Constraints, Journal of Thermal Stresses, 37(10), 1153-1172.

Tanigawa, Y., Jeon, S. P., and Hata, T. (1997). Analytical development of axisymmetrical elastic problem for semi-infinite body with Kassir's nonhomogeneous material property, The Japan Society of Mechanical Engineers, 63(608), 742–749.

Appendix A

Consider the differential equation

$$z^2\theta'' + z\theta' + \gamma^2\theta = 0, \quad z \in [h_1, h_2],\ h_1 > 0,\ h_2 > 0, \tag{A1}$$

with boundary conditions

$$\begin{aligned} &\theta = 0, \qquad at\ z = h_1, \\ &\theta = 0, \qquad at\ z = h_2. \end{aligned} \tag{A2}$$

The general solution of (A1) is given by

$$\theta(z) = C_1 \cos(\gamma \log z) + C_2 \sin(\gamma \log z),\ z > 0. \tag{A3}$$

where C_1 and C_2 are arbitrary constants.

To obtain the solution of (A1) that satisfies conditions (A2), we have

$$C_1 \cos(\gamma \log h_1) + C_2 \sin(\gamma \log h_1) = 0, \tag{A4}$$

$$C_1 \cos(\gamma \log h_2) + C_2 \sin(\gamma \log h_2) = 0. \tag{A5}$$

From (A4) and (A5), we get

$$\begin{aligned} &\frac{C_1}{C_2} = -\tan(\gamma \log h_1), \\ &\frac{C_1}{C_2} = -\tan(\gamma \log h_2). \end{aligned} \tag{A6}$$

Then, the function given by (A3) is a solution of (A1) subject to conditions (A2), if γ is a root of the transcendental equation

$$\sin(\gamma \log h_1)\cos(\gamma \log h_2) - \sin(\gamma \log h_2)\cos(\gamma \log h_1) = 0. \tag{A7}$$

Hence, we take $\gamma_i (i = 1, 2, 3, ...)$ to be the real and positive roots of equation (A7)

From equation (A4) and (A5), we have

$$\theta_i(z) = \frac{C_1}{\sin(\gamma_i \log h_1)}\left[\cos(\gamma_i \log z)\sin(\gamma_i \log h_1) - \sin(\gamma_i \log z)\cos(\gamma_i \log h_1)\right], \tag{A8}$$

$$\theta_i(z) = \frac{C_1}{\sin(\gamma_i \log h_2)}\left[\cos(\gamma_i \log z)\sin(\gamma_i \log h_2) - \sin(\gamma_i \log z)\cos(\gamma_i \log h_2)\right], \tag{A9}$$

We define

$$Z_i = \sin(\gamma_i \log h_1) + \sin(\gamma_i \log h_2),$$
$$W_i = \cos(\gamma_i \log h_1) + \cos(\gamma_i \log h_2).$$

Then,

$$S(\gamma_i z) = Z_i \cos(\gamma_i \log z) - W_i \sin(\gamma_i \log z). \tag{A10}$$

is taken to be the solution of (A1) - (A2).

By Sturm-Liouville theory (Birkoff and Rota 1989), the functions of the system (A10) are orthogonal on the interval $[h_1, h_2]$ with weight function z, that is

$$\int_{h1}^{h2} z\, S(\gamma_i z) S(\gamma_j z)\, dz = \begin{cases} S(\gamma_i), & i = j, \\ 0, & i \neq j, \end{cases} \tag{A11}$$

where $S(\gamma_i) = \left\| \sqrt{z} S(\gamma_i z) \right\|_2^2$, is the weighted L^2 norm.

If a function *f(z)* and its first derivative are piecewise continuous on the interval $[h_1, h_2]$, then the relation

$$T[f(z), h_1, h_2; \gamma_i] = \bar{f}(\gamma_i) = \int_{h1}^{h2} z\, f(z) S(\gamma_i z)\, dz, \tag{A12}$$

defines a linear integral transform.

To derive the inversion formula for this transform, let

$$f(z) = \sum_{i=1}^{\infty} [a_i\, S(\gamma_i z)]. \tag{A13}$$

On multiplying equation (A13) by $z\, S(\gamma_i z)$ and integrating both sides with respect to z, we obtain the coefficients as

$$a_i = \frac{1}{S(\gamma_i)} \int_{h1}^{h2} z\, f(z) S(\gamma_i z)\, dz = \frac{\bar{f}(\gamma_i)}{S(\gamma_i)}; \quad i = 1, 2, 3, ... \tag{A14}$$

Hence, the inversion formula becomes

$$f(z) = \sum_{i=1}^{\infty} \frac{\bar{f}(\gamma_i)}{S(\gamma_i)} S(\gamma_i z). \tag{A15}$$

Transform of the Differential Operator

We derive the transform of the following operator

$$D\,f(z)=\frac{d^2}{d\,z^2}\,f(z)+\frac{1}{z}\frac{d}{d\,z}\,f(z)+\frac{\gamma^2}{z^2}\,f(z);\ z\in[h_1,h_2]. \tag{A16}$$

Let I be the transform of first two terms of D, that is

$$I=\int_{h1}^{h2} z[\,f''(z)+(1/z)\,f'(z)]S(\gamma_i z)\,dz.$$

On solving I, we get

$$I=z[\,f'(z)S(\gamma_i z)-\gamma_i\,f(z)S'(\gamma_i z)]\Big|_{h1}^{h2}+\int_{h1}^{h2} z^{-1}[\gamma_i^2 z^2 S''(\gamma_i z)+\gamma_i z S'(\gamma_i z)]\,f(z)\,dz. \tag{A17}$$

Since S satisfies equation (A1), we have

$$\gamma_i^2 z^2 S''(\gamma_i z)+\gamma_i z\,S'(\gamma_i z)=-\gamma_i^2 S(\gamma_i z),$$

and

$$\int_{h1}^{h2} z^{-1}[\gamma_i^2 z^2 S''(\gamma_i z)+\gamma_i z\,S'(\gamma_i z)]\,f(z)\,dz=\int_{h1}^{h2} z[-\gamma^2/z^2]\,f(z)\,S(\gamma_i z)dz.$$

Also from (A2), we get

$$S(\gamma_i h_1)=S(\gamma_i h_2)==0,$$

Hence,

$$I=h_2\,S(\gamma_i h_2)\,f(h_2)-h_1\,S(\gamma_i h_1)\,f(h_1)-\gamma_i^2\,\bar{f}(\gamma_i)+T[-\gamma^2/z^2]\,f(z).$$

Therefore,

$$T[D\,f(z)]=h_2\,S(\gamma_i h_2)\,f(h_2)-h_1\,S(\gamma_i h_1)\,f(h_1)-\gamma_i^2\,\bar{f}(\gamma_i). \tag{A18}$$